Fracture Property Studies of Paracetamol Single Crystals Using Microindentation Techniques

Korlakunte V. R. Prasad,[1,2] David B. Sheen,[1] and John N. Sherwood[1,3]

Received February 1, 2001; accepted February 25, 2001

Purpose. To study the fracture behavior of the major habit faces of paracetamol single crystals using microindentation techniques and to correlate this with crystal structure and molecular packing.

Methods. Vicker's microindentation techniques were used to measure the hardness and crack lengths. The development of all the major radial cracks was analyzed using the Laugier relationship and fracture toughness values evaluated.

Results. Paracetamol single crystals showed severe cracking and fracture around all Vicker's indentations with a limited zone of plastic deformation close to the indent. This is consistent with the material being a highly brittle solid that deforms principally by elastic deformation to fracture rather than by plastic flow. Fracture was associated predominantly with the (010) cleavage plane, but was also observed parallel to other lattice planes including (110), (210) and (100). The cleavage plane (010) had the lowest fracture toughness value, K_c = 0.041MPa $m^{1/2}$, while the greatest value, K_c = 0.105MPa $m^{1/2}$ was obtained for the (210) plane.

Conclusions. Paracetamol crystals showed severe cracking and fracture because of the highly brittle nature of the material. The fracture behavior could be explained on the basis of the molecular packing arrangement and the calculated attachment energies across the fracture planes.

KEY WORDS: paracetamol; single crystal; microindentation; fracture toughness.

INTRODUCTION

The science of fracture mechanics was developed to determine the fundamental material properties that control fracture behavior, and to define its relationship with structural properties and mechanical constraints (1). The fracture strength of a material is characterized by the critical stress intensity factor, K_{IC}, which describes the state of the stress around an unstable crack or flaw in a material and is an indication of the stress required to produce catastrophic propagation of the crack. It is thus a measure of the resistance of a material to cracking.

A knowledge of the fracture properties of pharmaceutical materials is important in our understanding of how a material behaves during processes such as compaction and comminution. Fundamental to the understanding of such processes is knowledge of the fracture behavior of single crystals.

Most common methods used to measure the critical stress intensity factor for compressed pharmaceutical powders are three- or four-point bending (single edged notched beam (SENB) test), double torsion, and radial-edge cracked tablet tests (2). With the exception of the tablet tests, these require large specimens and careful sample preparation.

Microindentation testing techniques are finding increasing application in the study of mechanical properties especially in the assessment of the fracture behavior of brittle solids (3–6). The methods have certain advantages over other testing methods. They can be used on small single crystals, specimen preparation is relatively simple, and the indentation hardness and Young's modulus can be determined simultaneously. The techniques yield the fracture toughness, K_c, which is defined as the critical stress intensity factor for tensile fracture under plane stress conditions. The assessment of fracture toughness by the above technique is strictly semi-empirical because the analytical solutions of the stress field around indentations have not been solved; only approximate solutions have been derived, and the deformation field is not homogeneous and anisotropy and fracture complicate the problem. It is, however, a simply obtained and satisfactory diagnostic for the inter-comparison of the fracture behavior of materials.

As far as we are aware, there are few reports of the evaluation of the fracture toughness of single crystals of pharmaceutical materials using microindentation techniques (7–9).

Paracetamol powder compaction both alone and in the presence of excipients has been investigated by a number of researchers (10). Paracetamol has poor compression properties because of its high elastic recovery and resistance to plastic deformation (11). This causes it to fragment intensively during compaction. Despite the knowledge of these difficulties, which can lead to "capping" and the expression of included solvent, limited deformation and no detailed studies on the fracture behavior of single crystals have been reported for this material. Duncan-Hewitt and Weatherly (7) have reported the hardness, Young's modulus, and fracture toughness values as 421 MPa, 8.3GPa and 0.05 $MPam^{1/2}$, respectively for paracetamol single crystals. No indication is given of the crystal faces on which these measurements were made. In the present paper, we report a detailed study of the fracture behavior of various habit surfaces and evaluate the fracture toughness for the major fracture planes of paracetamol. The plastic deformation characteristics of this material are discussed in an accompanying publication (12).

MATERIALS AND METHODS

Crystal Growth

Large (5–10mm) single crystals of paracetamol were grown from commercially available material (Rhone Poulenc–Rhodapap, UK) by slow evaporation of a saturated solution of ethanol or water at 23°C over a period of 3–6 weeks. The crystals were harvested and dried quickly using soft tissue paper. Crystals were of either columnar habit with major {110} faces or tablet-like with major {001} faces. The predominant faces for the columnar form in order of morphological importance were {110} > {001} > {20$\bar{1}$} > {011} and for the

[1] Department of Pure and Applied Chemistry, University of Strathclyde, Glasgow G1 1XL, Scotland, UK.

[2] Present Address: PowderJect Centre for Gene and Drug Delivery Research, 43 Banbury Road, Dept. of Engineering Science, University of Oxford, Oxford OX2 6PE, England, UK.

[3] To whom correspondence should be addressed. (e-mail: j.n.sherwood@strath.ac.uk)

tablet-like crystals were {001} > {110} {011} > {20$\bar{1}$} > {100} (Fig. 1). These habits correspond to those reported in the literature and reflect growth under conditions of medium and high supersaturations respectively (13). These forms differ considerably from that of the crystals used by Duncan-Hewitt and Weatherly (14) in their previous study of this material.

Microindentation Testing

Microhardness indentation testing was performed with a Leitz Wetzlar Miniload 2 (Germany) hardness tester using a Vickers indenter at loads ranging from 0.049–0.392N. A dwell time of 30s was used in all tests. The temperature at which the tests were carried out was ~23°C.

The crystals were mounted on a glass microscope slide using a double-sided adhesive tape, so that the surface to be indented was normal to the indentation direction. This was achieved by orienting the microscope stage to maximise the intensity of light reflected from the surface when the crystal was viewed under the microscope attachment. The 50x objective was then used to select the indentation site. In the present work, the fracture anisotropy was determined from Vickers indentations made on fresh {001}, {20$\bar{1}$}, {110}, and {011} habit surfaces and on freshly cleaved {010} surfaces. The diagonals of the indentations were oriented parallel to or rotated 45° from the edges of the crystals. Care was taken to analyse only symmetrical impressions. Residual impression sizes and crack lengths were measured using the Miniload tester and the digital measuring eyepiece of the tester, which was recalibrated daily. Each hardness value and crack length used in the calculation is the mean of 20–30 indentations made on each of the habit faces of 3–4 crystals (Table I). The impressions were examined and photographed using a Leica Reichert Polyvar 2 microscope (Austria) having both incident and transmitted light capabilities. In carrying out the experiments and their analysis we adhered to the safeguards noted by Duncan-Hewitt and Weatherly (14).

Analysis of the Orientation and Disposition of Crack Traces

The orientation of radial crack traces originating at hardness impressions was determined by plotting the traces on an appropriate stereographic projection of the plane poles. Lines drawn orthogonal to the traces yielded sets of candidate crack planes. The exact orientations were identified with the help of transmitted light photomicrographs that showed the inclination of each particular plane to the surface.

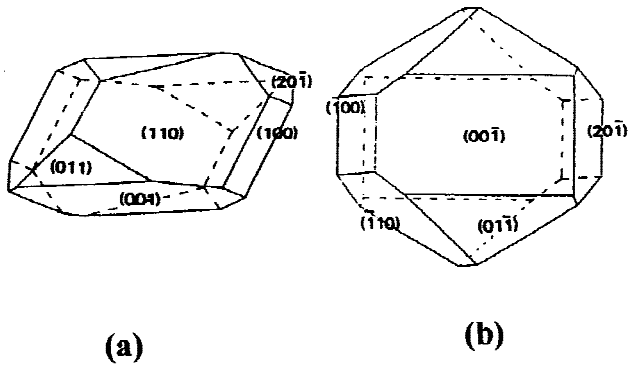

Fig. 1. Schematic morphologies of (a) columnar and (b) plate-like crystals of paracetamol grown from aqueous solution at medium (s = 7–11%) and high (s > 11%) supersaturations, respectively.

RESULTS

The Dependence of Fracture on Load for the {001} and {20$\bar{1}$} Surfaces

Examination of the influence of load on fracture was made on the {001} and {20$\bar{1}$} habit faces. Since the general behavior was similar in both cases, only the results for {001} are presented (Fig. 2a–e). From the figure it will be seen that radial cracks appear at the lowest load (0.049N), not only along the (010) cleavage plane, but also on other planes; in this case the (210) and (110) planes. These cracks increase in length with increasing load and are accompanied at higher loads by severe in-plane fracture to form lateral cracks and chipping. The lateral cracks appear as light halos and lie parallel to the (001) plane.

The behavior of the remaining faces is shown for a constant load of 0.147 N so that the surface cracking, which inevitably occurred at higher loads, did not obscure the fracture pattern.

Fracture Behavior

{001} Surfaces

Fracture behavior on {001} surfaces appeared to be anisotropic. When the indenter diagonal was aligned parallel to the [100] or [010] directions, the cracking occurred from three corners of the indenter and as well as from its edges (Fig. 3a and b). Faint slip traces were observed running parallel to the [100] direction (Fig 3a). The dominant crack appeared to be normal to the indentation surface and parallel to the cleavage plane (010). The other two major cracks which emanated from the opposite corners of the indenter, lay at an angle to the surface. From the stereographic projection of the (001) plane, these appeared to be directed along the family of (210) planes. Small secondary radial cracks emanating from the edges of the indentation probably belong to the family of (110) planes.

When the indenter was aligned at 45° to either of the [100] or [010] directions, the cracking occurred from the four corners and the edges of the indenter (Fig. 4 a and b). All the cracks lay at an angle to the indented surface. The transmitted light micrograph (Fig. 4b) reveals that the radial cracks are not in the halfpenny geometry (6) but are of the surface-localized Palmqvist type. In this indenter position, the cracking occasionally occurred parallel to the (010) plane. The major cracks were identified as being associated with the family of {110} planes. The fracture behavior appeared to be quite complicated when the indenter was aligned at 45° to the [010] direction.

{20$\bar{1}$} Surfaces

On the {20$\bar{1}$} face, when the indenter was aligned either parallel to or at 45° to the [010] direction, the cracking invariably occurred along the cleavage plane (Fig. 5a and b). The cracks always initiated at both of the opposite corners or

Table I. Fracture Toughness Values for Paracetamol Crystals

Fracture plane	Indentation plane	Crack length, c (μm) and crack type	Fracture toughness K_c, (MPa $m^{1/2}$)	Attachment energy, E_{at} (k cal.mol^{-1})	Slice energy, E_{sl} (k cal.mol^{-1})
(010)	(001)	39 ± 2; Radial	0.043 ± 0.007	−5.30	−18.05
	(110)	36 ± 2; Radial	0.048 ± 0.008		
	(201)	41 ± 2; Radial	0.041 ± 0.005		
	(011)	38 ± 2; Radial	0.043 ± 0.005		
	(010)	25 ± 2; Lateral	0.050 ± 0.008		
(210)	(001)	26 ± 2; Radial	0.105 ± 0.008	−15.30	−9.75
(110)	(001)	35 ± 2; Radial	0.052 ± 0.006	−10.00	−13.36
	(011)	30 ± 3; Radial	0.085 ± 0.0010		
(011)	(110)	30 ± 3; Radial	0.060 ± 0.010	−11.09	−12.27
(100)	(010)	25 ± 2; Radial	0.076 ± 0.010	−6.56	−16.79

edges of the indenter. Some strong slip traces were also observed running parallel to the (010) crack. These slip traces were more prominent when the indenter was parallel to the [010] direction. Some small secondary radial cracks were also noted and which lay in the family of (110) planes.

{110} Surfaces

Fracture on the {110} surfaces occurred in a similar way when the indenter was aligned either parallel to or at 45° with respect to the face edge (Fig 6). Half-circle halo lateral cracks

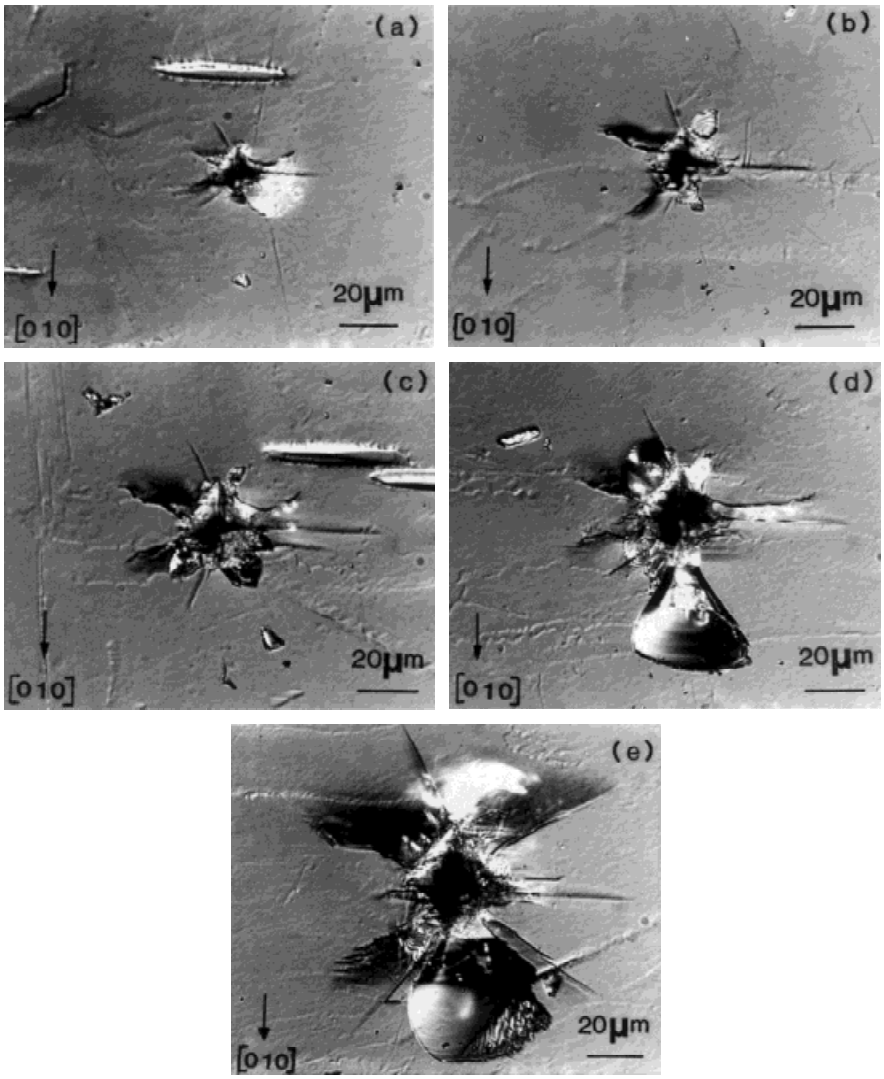

Fig. 2. Reflection photomicrographs of Vickers indentations on the {001} faces of paracetamol showing the fracture behavior at various loads [(a) 0.049N, (b) 0.147N , (c) 0.196N , (d) 0.294N, and (e) 0.392N].

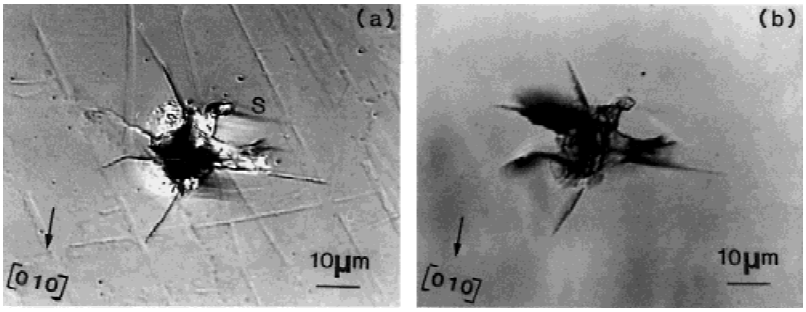

Fig. 3. (a) Reflection and (b) transmission photomicrographs of a Vickers indentation showing the fracture behavior on the {001} face of paracetamol (applied load = 0.147N). (the letter 's' represents the slip traces).

along with radial cracks emanated from the edges of the indenter. The radial cracks, identified as (010) cracks, always appeared parallel to the [001] direction and lay at an angle to the (110) plane.

{011} Surfaces

The fracture behavior on the {011} surface was the same whether the indenter was parallel to or at 45° from the edges and comprised large semicircular, subsurface lateral cracks, and major and minor radial cracks. The major radial crack was identified as a (010) fracture plane, which crystallographically should lie at about 55° to the surface. The minor radial cracks were identified as (100) and (110) fracture planes. The subsurface lateral crack was identified as (011).

{010} Cleavage Plane

The (010) cleavage face was found to be the most difficult to indent. It always yielded a subsurface lateral crack, observable as a bright halo feature in incident light illumination. This surrounded the indentation impression and was accompanied by some radial cracks emanating from the corners and the edges of the indentation. The subsurface lateral crack corresponded to a (010) crack surface and the radial crack corresponded to a (100) crack surface.

Plastic Deformation

In addition to deformation by fracture there was also a distinct indication of prior plastic deformation. This was evidenced by the formation of slip traces (noticeable particularly in Fig. 5a and 3a) in the vicinity of the indentation. These aligned along the intersection of the (010) plane with the surface and presumably represent dislocation slip on a (010) slip plane. This was confirmed by etching, which showed the slip traces to comprise etch pits and hence dislocation alignments (12). The minimal extent of these slip traces implies a very limited plasticity in this material. This conclusion is supported by the clarity of the hardness impressions which show none of the barrelling or pincushioning associated with significant plastic flow.

Fracture Toughness Assessment

The fracture toughness values K_c were calculated as a function of load, from the lengths of cracks emanating from the microindentations. On the basis of the configuration of the resulting crack patterns, the formula used for the radial cracks was that proposed by Laugier (15) which assumes that the cracks possess a configuration similar to that described by Palmqvist (16):

$$K_c = K_p\,(a/l)^{0.5}(E/H)^{0.67}\,(P/(c)^{1.5}) \qquad (1)$$

For similar reasons, those for subsurface lateral cracks were calculated using the formula developed by Marshall, Lawn and Evans (17):

$$K_c = 0.012\,E^{3/4}(1/H)(P/(c)^{1.6})^{5/4}. \qquad (2)$$

Where a is the half-diagonal of the indentation (m), c is the crack length (m), H is the Vickers hardness (MPa), P is the indenter load, (MN), l = c – a, E is the Young's modulus (10.9 Gpa), and K_p is a constant (0.015). The dependency of the power law ($c \alpha P^{2/3}$) required for the Laugier correlation, was verified within reasonable limits for the cracks observed on the two major faces {001} and {201} over the load range used (Fig. 7).

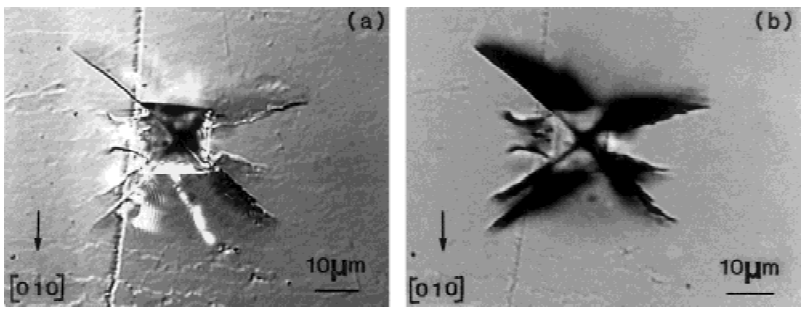

Fig. 4. (a) Reflection and (b) transmission photomicrographs of a Vickers impression on the {001} face of paracetamol showing radial cracks (applied load = 0.147N).

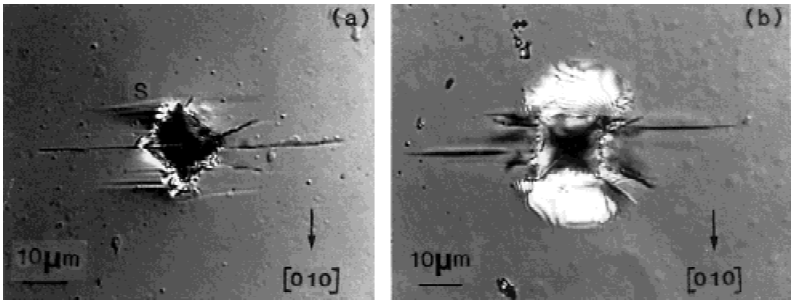

Fig. 5. Reflected light photomicrographs of a Vickers impression (0.147N load) showing radial cracks and some slip traces on {20$\bar{1}$} surfaces (a) indenter diagonal aligned parallel to [010] direction and (b) indenter diagonal rotated 45° to the [010] direction.

DISCUSSION

From Table I we see that the fracture toughness is greatest across (210) and least across (010) which accounts for the dominance of (010) plane in the fracture hierarchy and its position as the dominant cleavage plane in this material. The value of 0.041 MPa $m^{1/2}$ for fracture across (010) is close to that reported by Duncan-Hewitt and Weatherly (0.05 MPa $m^{1/2}$) (7). The remaining listed fracture planes and their toughness values have not been reported previously.

A direct impression of the relative ease of fracture along the various fracture planes can be gained from the molecular geometry of the crystal lattice. Figure 8 shows the {001} surface and indicates on this the position of the three major fracture planes (010), (210), and (110). The relative potential for fracture is immediately obvious.

Since significant molecular fracture is forbidden, the (010) plane follows a serrated path across which there are no hydrogen bonds and hence interplanar bonding is purely of van der Waals type (Fig. 8). In plane, however, the intermolecular bonding is stronger.

Fracture along both (110) and (210) requires the breakage of two hydrogen bonds per unit cell and for (210) a complicated trajectory to avoid molecular breakage. The (100) fracture would be similarly affected. Thus from this simple structural approach it is not surprising that (010) is a cleavage plane and the remainder fracture planes of increasing fracture toughness.

To move closer to a predictive model, this relationship can be quantified in terms of the in-plane and inter-plane forces that can be calculated from knowledge of the structural and intermolecular force field parameters for the material.

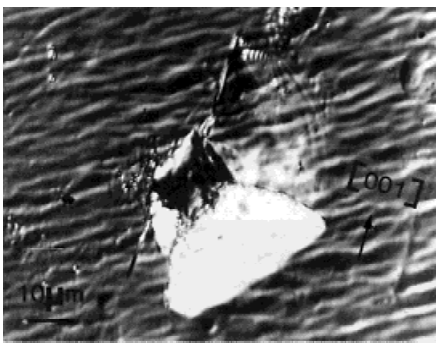

Fig. 6. Reflected light photomicrographs of a Vickers impression on the {010} cleavage surface of paracetamol (0.147N load) showing subsurface lateral cracks and radial cracks.

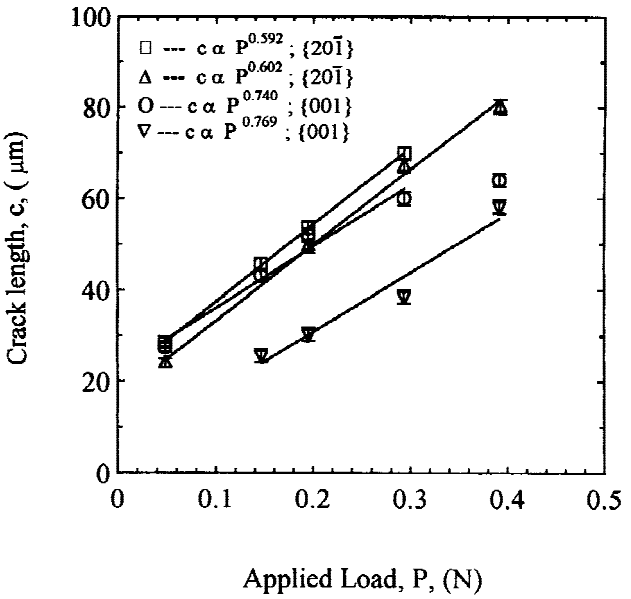

Fig. 7. Variation of Crack Length (c) with Applied Load (P) for the {001} and {20$\bar{1}$} faces of paracetamol.

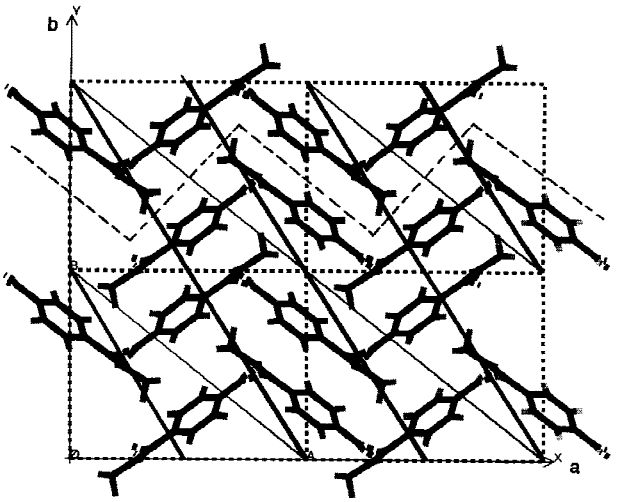

Fig. 8. Molecular packing on the **ab** plane of monoclinic paracetamol. The serrated dotted line indicates the position of the (010) cleavage plane. The fine and thick diagonal lines represent the (110) and (210) planes respectively.

Using a well tried computer modelling programme (HABIT 95) with suitable intermolecular potentials, values of the attachment energy of sequential molecules or planes to the surfaces and in-plane surface slice energies can be evaluated (18–20). We have made such an evaluation for typical habit faces of paracetamol using a MOMANY (21) molecular potential. This potential is particularly applicable to systems such as the present in which both van der Waals and hydrogen bonding interactions are important as cohesive forces in the crystal. It includes well-developed routines for addressing both types of interaction.

The resulting values are included in Table I and show the potential merit of such comparisons as pointers in a predictive analysis. The attachment energy E_{att} and slice energy E_{slice} are respectively minimum and maximum for the (010) planes relative to other fracture planes and non fracture planes for which our analysis has been developed. Whether or not such an analysis can be extended to include comparison with other materials is open to question. There is no guarantee of the broad applicability of the intermolecular potentials or the comparison between different sets of data each evaluated from the different potentials that are appropriate to each case. Much remains to be done but we hope to test this basic applicability as we extend the range of materials examined.

CONCLUSIONS

Paracetamol crystals showed severe cracking and fracture because of the highly brittle nature of the material. The fracture behavior was found to be anisotropic for {001} surfaces and depended on the orientation of the indenter. The remaining faces showed a more isotropic fracture behavior. The fracture toughness was lowest for the (010) cleavage plane and highest for the non-habit (210) plane. The fracture behavior for paracetamol can be explained on the basis of the molecular packing and interplanar forces (attachment energies) in the structure.

ACKNOWLEDGMENTS

We gratefully acknowledge the financial support of this work by the UK EPSRC and the three pharmaceutical companies; Pfizer, Roche, and SmithKline Beecham. The work was carried out as part of a programme entitled "Particle Formation, Processing and Characterisation for the Pharmaceutical Industry involving" the Universities of Bradford, Strathclyde, and Surrey. We also acknowledge the kindness of Dr R Hammond of Heriot-Watt University in providing supplementary data on the energetics of molecular attraction in the paracetamol crystal lattice.

REFERENCES

1. B. R. Lawn and T. R. Wilshaw. *Fracture of Brittle Solids*. Cambridge University Press, Cambridge, 1975.
2. R. C. Rowe and R. J. Roberts. Mechanical Properties. In G. Alderborn and C. Nystrom (eds.), *Pharmaceutical Powder Compaction Technology*, vol. 71, Marcel Dekker, New York, 1996 pp. 283–322.
3. B. R. Lawn and T. R. Wilshaw. Indentation fracture: Principles and applications. *J. Mater. Sci.* **10**:1049–1081 (1975).
4. B. R. Lawn and M. V. Swain. Microfracture beneath point indentations in brittle solids. *J. Mater. Sci*. **10**:113–122 (1975).
5. G. R. Anstis, P. Chantikul, B. R. Lawn, and D. B. Marshall. A critical evaluation of indentation techniques for measuring toughness: I, direct crack measurements. *J. Am. Ceram. Soc*. **64**:533–538 (1981).
6. R. F. Cook and G. M. Pharr. Direct observation and analysis of indentation cracking in glasses and ceramics. *J. Am. Ceram. Soc*. **73**:787–817 (1990).
7. W. C. Duncan-Hewitt and G. C. Weatherly. Evaluating the hardness, Young's modulus and fracture toughness of some pharmaceutical crystals using microindentation techniques. *J. Mater. Sci. Lett*. **8**:1350–1352 (1989).
8. W. C. Duncan-Hewitt and G. C. Weatherly. Evaluating the deformation kinetics of sucrose crystals using Microindentation techniques. *Pharm. Res.* **6**:1060–1066 (1989).
9. W. L. Elban, D. B. Sheen, and J. N. Sherwood. Vickers hardness testing of sucrose single crystals. *J. Cryst. Growth* **137**:304–308 (1994).
10. G. K. Bolhuis and Z. T. Chowan. Materials for direct compaction. In G. Alderborn and C. Nystrom (eds.), *Pharmaceutical Powder Compaction Technology*, vol. 71, Marcel Dekker, New York, 1996 pp. 419–500.
11. M. E. Aulton, H. G. Tebby, and P. J. P. White. Indentation hardness testing of tablets. *J. Pharm. Pharmacol*. **26**(Suppl):138P, (1974).
12. S. Finnie, K. V. R. Prasad, R. I. Ristic, D. B. Sheen, and J. N. Sherwood. Microhardness and dislocation identification studies on paracetamol single crystals. *Pharm. Res.* **18**:674–681 (2001).
13. S. Finnie, R. I. Ristic, J. N. Sherwood, and A. M. Zikic. Characterisation of growth behavior of small paracetamol crystals grown from pure solutions. *Trans. I. Chem E.* **74A**:835–838 (1996).
14. W. C. Duncan-Hewitt, D. L. Mount, and A.Yu. Hardness anisotropy of acetaminophen crystals. *Pharm. Res.* **11**:616–623 (1994).
15. M. T. Laugier. New formula for indentation toughness in ceramics. *J. Mater. Sci. Lett*. **6**:355–356 (1987).
16. S. Palmquist. The work for the formation of a crack during Vickers indentaion as a measure of the toughness of hard metals (in Ger.). *Arch. Eisenhüttenwiss.* **33**:629–634 (1962).
17. D. B. Marshall, B. R. Lawn, and A. G. Evans. Elastic/plastic indentation damage in ceramics: The lateral crack system. *J. Am. Ceram. Soc*. **65**:561–566 (1982).
18. G. Clydesdale, R. Docherty, and K. J. Roberts. HABIT—A programme for predicting the morphology of molecular crystals. *Comput. Phys. Commun*. **64**:311–328 (1991).
19. G. Clydesdale, K. J. Roberts, and R. Docherty. HABIT 95—A program for predicting the morphology of molecular crystals as a function of the growth environment. *J. Cryst. Growth* **166**:78–83 (1996)
20. H. G. Gallagher, K. J. Roberts, J. N. Sherwood, and L. A. Smith. A theoretical examination of the molecular packing, intermolecular bonding and crystal morphology of 2,4,6-trinitrotoluene in relation to polymorphic structural stability. *J. Mater. Chem*. **7**: 229–235 (1997).
21. F. A. Momany, R. F. McGuire, A. W. Burgess, and H. A. Scheraga. Energy parameters in polypeptides. VII Geometric parameters, partial atomic charges,non-bonded interactions and intrinsic torsional potentials for the naturally occuring amino acids. *J. Phys. Chem*. **79**:2361–2381 (1975).